Massive gauge theory with quasigluon for hot $SU(N)$: Phase transition and thermodynamics

Jiang Zhu* and Zhao-feng Kang‡
School of Physics, Huazhong University of Science and Technology, Wuhan 430074, China

Jun Guo†
College of Physics and Communication Electronics, Jiangxi Normal University, Nanchang 330022, China

(Received 24 November 2022; accepted 22 February 2023; published 7 April 2023)

It is challenging to build a model that can correctly and unifiedly account for the deconfinement phase transition and thermodynamics of the hot $SU(N)$ pure Yang-Mills (PYM) system, for any N. In this article, we slightly generalize the massive PYM model to the situation with a quasigluon mass $M_g(T)$ varying with temperature, inspired by the quasigluon model. In such a framework, we can acquire an effective potential for the temporal gauge field background by perturbative calculation, rather than adding by hand. The resulting potential works well to describe the behavior of the hot PYM system for all N, via the single parameter $M_g(T)$. Moreover, under the assumption of unified eigenvalue distribution, the $M_g(T)$ fitted by machine learning is found to follow N-universality.

DOI: 10.1103/PhysRevD.107.076005

I. INTRODUCTION

To build a model that can describe the deconfinement phase transition of the $SU(N)$ PYM system at finite temperature, which is hampered by the nonperturbative effect, one should first figure out what knowledge we have about such a system. In the very high-temperature region, it should recover the Stefan-Boltzmann (SB) limit, following the asymptotic freedom of the non-Abelian gauge theory. The more crucial information comes from the lattice simulations, which provide a reliable way to deal with strong coupling, thus furnishing the order of deconfinement phase transition and as well data of thermodynamic observables, such as pressure and the latent heat L.[1] The deconfinement phase transition is a crossover for $N = 2$ and FOPT for $N \geq 3$. Moreover, combining the data for pressure and the latent heat allows us to extract the following large N scaling law [1]

$$p_M = \frac{M^2-1}{N^2-1}\, p_N, \qquad L_M = \frac{M^2-1}{N^2-1} L_N, \tag{1.1}$$

where N and M represent different color number. It is challenging to build a model with strong theoretic ground that can correctly account for all of the above aspects of the hot PYM system, for any N beyond $N = 3$. However, it is very meaningful, not only in the theoretical sense but also in the application to the new physics domain, where an (almost) pure $SU(N)$ gauge sector receives wide interest [7–12]. Recently, the prospects of gravitational wave signals during the deconfinement phase transition are studied based on different models [1–4,13,14].

The popular line is following the Z_N center symmetry and the traced Polyakov loop (PL) as order parameter, to construct effective PL models, usually, the polynomial models [1,4,15,16] also see review [17]. Another line is underlined by the Haar measure, which gains great success in the $SU(3)$ case, even incorporating dynamic quarks [18–21]. For $SU(3)$ only, both types of model can describe the deconfinement phase transition and as well the thermodynamics, at least in the semi-QGP region. However, when we try to extend them to general $SU(N)$ cases, we encounter some difficulties. The Haar-type model is shown to be inconsistent with the above large N scaling law [1] and moreover, it cannot be handled for very large N. The polynomial model proposed in Refs. [1,4] utilizes the competition among terms with designed powers and signs to realize the deconfinement phase transition. Since it basically respects just a Z_2 symmetry and thus works for any N, even including $N = 2$. The matrix models, inspired by

*jackpotzhujiang@gmail.com
†jguo_hep@163.com
‡zhaofengkang@gmail.com

[1]The latent heat is not only important to describe the first-order phase transition (FOPT) but also critical in cosmology because the gravitational-wave produced during the deconfinement phase transition in the early universe is directly related to this quantity [1–6].

the property of perturbation potential, instead [22–25] treat the eigenvalues of the thermal Wilson line as fundamental variables, which may provide a feasible way to understand the behavior of the hot PYM system for all N. Largely speaking, these models are phenomenally oriented, lacking a more profound basis to derive the shape of the thermodynamic potential.

As long as only thermodynamics is concerned, the quasiparticle model (QPM) is even more attractive. It is a statistical model where the gluons are assumed to develop a temperature-dependent mass, due to the nonperturbative interaction with the thermal environment. This picture is strongly supported by the hard-thermal-loop perturbation theory at high-temperature regions [26]. It can successfully explain the thermodynamics of the hot $SU(N)$ PYM system from T_c to the SB limit [27–30]. Later, taking into account the temporal gauge field background A_0 brings a difference [23] and opens the possibility to describe both thermodynamics and the deconfinement phase transition at the same time. But most studies of the interplay between quasigluon and background focus on the modification to the pressure of hot PYM, the critical nonperturbative dynamics driving the deconfinement phase transition, says the Haar measure term, is still added by hand and external to the QPM picture [31–33]. This might be contradictory to the spirit of QPM, where most of the non perturbation interaction has already been "absorbed" into the quasiguon mass.

Although not a following study of QPM, the massive PYM model [34–36] shares a similar philosophy with QPM, and it also assumes that the effective gluon mass parameter simply encodes the nonperturbative effects. Then, the effective potential for the temporal background can be derived, instead of added by hand, at one loop level or even beyond [37,38]. This approach realizes the inverted Weiss potential, attributed to the enhanced ghost contribution, as the mechanism for the deconfinement phase transition. Surprisingly, for $N = 2$, the resulting effective potential indeed predicts a crossover instead of FOPT.

Thus, it is tempting to marry QPM with the massive PYM. The original massive PYM model [35] just takes a constant quasigluon mass, and now we generalize it to have temperature dependence, which is in line with the framework of hard-thermal-loop perturbation theory and may serve as a quantum field basis for the QPM. We find that the resulting one-loop effective potential indeed can successfully describe both the deconfinement phase transition and the thermodynamics of the hot PYM system, for any color number N. Our study is helpful to understand the deconfinement phase transition in cosmology.

The paper is organized as follows: We give a short review of the QPM in Sec. II and then goes to the generalized massive PYM according to the QPM in Sec. III, where we derive the effective potential at one loop and investigate the deconfinement phase transition with the assumption of uniform eigenvalue distribution, which reduces the potential to one-dimension. In Sec. IV we study thermodynamics from the critical temperature to the SB limit, fitting the quasigluon mass by lattice data via machine learning. Conclusions and discussions and as well as the appendix are cast in the remaining two sections.

II. QUASIGLUON: FROM HTL TO T_c

For thermal gauge theories at high temperature, the classical solution should not be described by the gluonic states without mass but with mass, which stems from the plasma effects such as the screening of electric fields and Landau damping. The hard-thermal-loop perturbation theory (HTLpt) [26], which is a reorganization of the perturbation series and can take into account the plasma effects consistently. It is found that at next-next-leading order, the hot gluon plasma can be well described by weakly coupled quasigluons down to $(2-3)T_c$ [39,40].

Within the HTLpt, the transverse quasigluon in the QCD medium follows the dispersion equation

$$w^2 - k^2 - \Pi_t^*(w,k) = 0, \tag{2.1}$$

where $\Pi_t^*(w,k)$ is the transverse self-energy for the hot gluons, having weak momentum dependence but strong temperature dependence. At leading order, it is given by [26]

$$\Pi_t^*(w,k) = \frac{N}{6} g^2 T^2, \tag{2.2}$$

with g the gauge coupling. The gluon quasiparticles mainly propagate on shell.

For even lower temperature, the magnetic/nonperturbative effects become important. But it is tempting to pursue the possibility that even down to T_c, the plasma can still be described by an ideal gas of "massive" noninteracting "gluons," where the strong interactions between gluon and the in-medium have been "absorbed," at least partially, into the quasigluon mass. Following this line, the authors of Refs. [27,29] explained the lattice QCD thermodynamics near T_c via a simple quasiparticle model (QPM) inspired by the above HTL quasiparticle. And to naturally match the HTLpt quasiparticle at high T, they simply consider such a QPM with quasigluon mass squared[2]

$$M_g^2(T) = \frac{N}{6} G^2(T) T^2, \quad G^2(T) = \frac{48\pi^2}{11N \log\left(\frac{T}{T_c/\lambda} + \frac{T_s}{T_c}\right)^2} \tag{2.3}$$

which parametrizes the deviation from HTLpt quasiparticle via the parameter T_s and λ. Other form of $M_g(T)$ is possible, for instance the one in Ref. [41].

[2]The quasigluon mass is determined by the pole of gluon self-energy in the complex momentum plane, but the exact location is hampered by the nonperturbative effect.

Then, such a pool of ideal quasi gluon gas, assumed to respect the Bose distribution f_B, has pressure

$$p(T) = \frac{g(T)}{6\pi^2}\int_0^\infty f_B(E_k)\frac{k^4}{E_k}dk - B(T), \tag{2.4}$$

with $E_k = \sqrt{k^2 + M_g^2(T)}$. Owing to the temperature dependence of mass, the self-consistent thermodynamic relation for ideal gas, namely the Gibbs-Duhem relation, $\epsilon + p = sT$ with $s = \partial p/\partial T$ is violated. Including $B(T)$ can solve this problem [30]. It is not independent and is determined by $M_g(T)$, up to a bag constant. Surprisingly, this simple QPM is capable of reproducing the quenched QCD or $SU(3)$ PYM lattice data in the whole region above T_c [29]. Study for other $N = 4$, 5, 6 is presented in Refs. [42,43]. It is common that, in order to reduce the contribution of quasigluons near the critical temperature, a very large quasigluon mass is usually required.

However, the original QPM is just a statistical model and thus cannot explain the order of $SU(N)$ phase transition. The latter is supposed to be understood in the framework of Landau phase transition: Find a proper order parameter η and construct a (coarse-grained) Landau free energy as a function of the order parameter, and then one can study the order of phase transition by surveying its ground state. In studying the deconfinement phase transition of $SU(N)$ PYM, the Polyakov loop (PL) associated with the center symmetry Z_N is identified with η; it is defined as $l_N = \mathrm{tr}\hat{L}_F/N$, the traced thermal Wilson line in the fundamental representation

$$\hat{L}_F = \mathcal{P}e^{ig\int_0^\beta A_4^a(x,t)t^a dt}, \tag{2.5}$$

with $\mathcal{P}$ denoting path ordering and t^a the generators of the fundamental representation for $SU(N)$.

III. QUASIPARTICLES MOVE IN THE PL BACKGROUND

So, it is a natural idea to combine quasiparticle model with PLM, to study the deconfinement phase transition dynamics and thermodynamics simultaneously [23,32].[3] In such models, quasigluons moving in the PL background generate thermodynamic potential which depends on the PL in the adjoint representation $\hat{L}_A$ [23]:

$$\Omega_{\mathrm{QG}}(\hat{L}_A, T) = 2T\mathrm{tr}\int\frac{d^3\vec{p}}{(2\pi)^2}\log(1 - \hat{L}_A e^{-E_g/T}). \tag{3.1}$$

It is a phenomenological generalization to the usual Weiss potential [44] for the fundamental gluons to quasigluons, by replacing $|\vec{p}|$ with $E_g = \sqrt{M_g(T)^2 + p^2}$. Later, we will derive a similarity grounded on the QFT, but with a remarkable difference. The quasigluons dominate thermodynamics in the high-temperature region, where $M_g \ll T$ and $\hat{L}_A \to 1$, explain the blackbody behavior. At the lower temperature, typically below $2T_c$, the decreasing PL combined with the increasing $M_g(T)$, is capable of explaining the deviation from the blackbody spectrum toward T_c [23,31–33,45].

But that is all. We cannot expect this part to give the deconfinement phase transition at the same time, which needs additional interaction, such as the van der Monde determinant interaction [23,31,33,46]. In this article, we follow another line proposed in Ref. [35], which enables us to study the nonperturbative PT in the perturbative approach; in their philosophy, nonperturbation effects are encoded in the gluon mass, in line with the QPM picture. In the following, we will first present an effective model, which is a slight generalization to that in Ref. [35]. Then, we reproduce the effective potential Eq. (3.1) as well as the confining potential from the model through the leading order thermal correction.

A. Effective model for quasigluon above T_c

The model in Ref. [35] quantizes PYM in the background field gauge formalism, including massive fluctuations. Then, the Faddeev-Popov gauge-fixed Lagrangian reads

$$\mathcal{L} = -\frac{1}{2g^2}\mathrm{tr}(F_{\mu\nu}F^{\mu\nu}) + \bar{D}_\mu\bar{c}^a D^\mu c^a + ih^a\bar{D}_\mu\hat{A}^{\mu,a} + \frac{1}{2}M_g^2(T)\hat{A}_\mu^a\hat{A}^{a,\mu}, \tag{3.2}$$

where $c, \bar{c}$ and h are the Ghost fields, real Nakanishi-Lautrup field, respectively. We have split the gauge field A_μ as $A_\mu = \bar{A}_\mu + \hat{A}_\mu$ with $\hat{A}_\mu$ the massive fluctuations. The background $\bar{A}_\mu$ is restricted to merely have the constant temporal component, $\bar{A}_\mu = \bar{A}_0\delta_{0\mu}$, for the sake of preserving invariance of the PYM system, under both temporal and spatial translations and spatial rotations at finite T. The covariant derivative acting on $\phi = (c, \bar{c}, h, \hat{A}_\mu)$ is defined as

$$\bar{D}_\mu^{ab} = \partial_\mu\delta^{ab} + gf^{acb}\bar{A}_\mu^c, \tag{3.3}$$

where the gauge field is the background field. The above Lagrangian has implemented the Landau-DeWitt gauge $\bar{D}_\mu\hat{A}^\mu = 0$. This gauge fixed PYM, including the gluon mass term, still respects the background local $SU(N)$ symmetry, with covariant derivative defined above and treating ϕ as adjoint matter fields.

In the effective model specified by Eq. (3.2), the gluon mass is not originally interpreted as quasigluon mass.

[3]This idea originated from an earlier work [22], although there the authors have not introduced quasigluon explicitly yet.

Instead, it is regarded as a gauge fixing parameter, to further remove the degeneracy among the Gribov copies, whose existence may make the Faddeev-Popov procedure in the deep infrared region invalid [47]. This region is associated with the nonperturbative dynamics of PYM. Hence, people hope that M_g at the same time can "absorb" strong interactions, so that some nonperturbation phenomena can be studied by the perturbation method. Such a philosophy is consistent with the QPM, and therefore it is tempting to simply identify M_g as the quasigluon mass, which is reasonable at least at zero temperature. If such a formalism is consistent with the Hamilton approach which establishes a QFT basis for quasiparticle [48], is open.

However, to explain thermodynamics, we need a temperature-dependent quasigluon mass, $M_g(T)$. This may be odd with the usual understanding of thermal mass origin in perturbative thermal QFT: The underlying Lagrangian is the same as that of $T=0$ and does not include the temperature-dependent quantity, and this kind of dependence originates from thermal correction. However, it is not strange that the Lagrangian includes a temperature dependent quantity. In fact, the HTL resummation scheme based on quasiparticle picture is just based on the effective Lagrangian including thermal mass, which gives rise to the modified propagator for the calculation of thermal corrections. Since we are extending the quasiparticle picture down to near T_c, we should naturally include the temperature-dependent quasigluon mass term.

Therefore, as a slight generalization to the model in Ref. [35], the effective Lagrangian Eq. (3.2) is supposed to furnish a phenomenological framework to perturbatively study deconfinement phase transition along with full thermodynamics above T_c.

B. The thermodynamic potential for quasiparticle model: Pure gluonic part

In this subsection, we will calculate the thermodynamic potential for the fundamental PL in a general PYM with gauge group $SU(N)$, following the textbook approach. That is to integrate out all fluctuations $\hat{A}_\mu = A_\mu - \bar{A}_\mu$ over the temporal background $\bar{A}_\mu = \bar{A}_0\delta_{0\mu}$, in the $3+1$ Euclidean QFT. For a homogeneous background, one can always make $\bar{A}_0$ diagonal via some global $SU(N)$ rotation. Therefore, we can expand $\bar{A}_0$ in the $su(N)$ Cartan space, which is spanned by the diagonal subgroup $\{H^i\}$ $(i=1,2,\ldots N-1)$ with $[H^i,H^j]=0$, and then $\bar{A}_0=\bar{A}_0^i H^i$ with $\bar{A}_0^i$ is the Cartan coordinates.

Let us first deal with the pure gluonic part of Eq. (3.2), from which one can get the quadratic Lagrangian of the fluctuation field $\hat{A}_\mu$

$$\mathcal{L}^{(2)} = -\frac{1}{2}\hat{A}_\mu^a[\delta_{ab}g^{\mu\nu}\partial^2 - f_{abc}(\partial^\nu\bar{A}^{\mu,c} + 2g^{\mu\nu}\bar{A}_\rho^c\partial^\rho) + f_{acd}f_{cbe}g^{\mu\nu}\bar{A}_\rho^d\bar{A}^{\rho,e} + 2f_{abc}\bar{F}^{\mu\nu,c}]\hat{A}_\nu^b. \tag{3.4}$$

It can be written as the following

$$\mathcal{L}^{(2)} = \frac{1}{2}\hat{A}_\mu^a(D^{-1})_{ab}\hat{A}^{\mu,b}, \tag{3.5}$$

with the operator defined as

$$(D^{-1})_{ab} = \delta_{ab}(p^2+M_g^2) + 2i\sum_i f_{abi}\bar{A}_0^i p_0 - \sum_{i,j} f_{aci}f_{cbj}\bar{A}_0^i\bar{A}_0^j. \tag{3.6}$$

The last term denotes the mass of the fluctuations (explained as the quasigluons) from the temporal background, and hence the background field will obtain a thermodynamic potential from the plasma of quasigluons.

Before we calculate this potential, let us deal with the propagator, diagonalizing the fluctuations in the color space through a unitary transformation. Then, the diagonal propagators takes the form of

$$\tilde{D}_{aa}^{-1}(p) = (p_0 - A_a)^2 + |\vec{p}|^2 + M_g^2. \tag{3.7}$$

Following the standard approach of path integral, one can get the generating function (Z below should be understood as Z^I, the gluonic part contribution, but for the sake of simplicity, we ignore the superscript, which we believe will not cause ambiguity)

$$\log\, Z = \frac{1}{2}\log\,\det\left[-\frac{\delta^2\mathcal{L}^{(2)}}{\delta A\delta A}\right] = \frac{1}{2}\log\,\det[D^{-1}] = \frac{1}{2}\log\,\det[\tilde{D}^{-1}]. \tag{3.8}$$

where we have used the property that unitary transformation does not change determinate. Then, using the trick that $\log\,\det A = \mathrm{Tr}\,\log A$ we get

$$\log\,\det[\tilde{D}^{-1}] = \mathrm{Tr}\,\log[\tilde{D}^{-1}]. \tag{3.9}$$

"Tr" is the trace over the functional propagator operator, and can be split into two parts: a function trace over momentum space and a color space trace denoted by "$\mathrm{tr_c}$", explicitly,

$$\mathrm{Tr}\,\log[\tilde{D}^{-1}] = \mathrm{tr_c}\int\frac{d^4p}{(2\pi)^4}\log[\tilde{D}^{-1}(p)]. \tag{3.10}$$

In order to get the finite temperature potential, one can discretize the energy by $p_0\to\omega_n = 2i\pi nT$ and transform $\bar{A}_0\to -i\bar{A}_4$, obtaining

$$\log Z = 2V\mathrm{tr_c}\int\frac{d^3\vec{p}}{(2\pi)^2}\sum_{n=-\infty}^{\infty}\log[\tilde{D}_{aa}^{-1}(\omega_n,|\vec{p}|)], \tag{3.11}$$

where V is the space volume and $2 = \frac{1}{2} \times 4$ with 4 denoting the multiplicity from the four components of A_μ. From Eq. (3.7), the structure of the propagator $\tilde{D}^{-1}(\omega_n, |\vec{p}|)$ takes the form of

$$\tilde{D}^{-1}_{aa}(\omega_n, |\vec{p}|) = (\omega_n - A_a)^2 + |\vec{p}|^2 + M_g^2, \tag{3.12}$$

where A_a is a linear combination of the background $\bar{A}^i_4$, with coefficients determined by the structure constant, but we do not find a general expression for any N yet. As a matter of fact, the concrete expression is not important in our discussion, since later we will switch to a parametrization of the background which is independent of A_a. Anyway, in Appendix B, we present the details of our calculation for $SU(4)$, and the procedure applies to other values of N.

The summation of the thermal excitation modes n can be done explicitly using a trick in Appendix C. And finally, the generating function can be compactly written as

$$\log Z = 4V\mathrm{tr}_c \int \frac{d^3\vec{p}}{(2\pi)^2} \log(1 - \hat{L}_A e^{-E_g/T}), \tag{3.13}$$

where $\hat{L}_A$ is expressed in terms of background field $\bar{A}_\mu$, and it is nothing but the PL in the adjoint representation. For instance, in $SU(3)$ it is given by

$$\hat{L}_A = \mathrm{diag}[1, 1, e^{i\bar{A}^3_4/T}, e^{-i\bar{A}^3_4/T}, e^{i(\bar{A}^3_4+\sqrt{3}\bar{A}^8_4)/2T}, e^{-i(\bar{A}^3_4+\sqrt{3}\bar{A}^8_4)/2T}, e^{i(\bar{A}^3_4-\sqrt{3}\bar{A}^8_4)/2T}, e^{-i(\bar{A}^3_4-\sqrt{3}\bar{A}^8_4)/2T}], \tag{3.14}$$

where we have written it in terms of the original background. It is seen that the temporal background behaves as an imaginary chemical potential. Equation (3.13) yields the effective potential $\mathcal{V}_{\mathrm{eff}} = \frac{T}{V}\log Z$ which almost recovers the generalized Weiss potential given in Eq. (3.1), up to the coefficient. But the ghost contribution, which will be included in the following subsection, will result in a substantial deviation related to the deconfinement potential.

Equation (3.14) demonstrates the general structure of thermal Wilson line in the adjoint representation, i.e., its elements are organized such that it can be rewritten in terms of the eigenphases of the fundamental thermal Wilson line [46]

$$\hat{L}_F = \mathcal{P}e^{ig\int_0^\beta A_4(x,t)dt} \to \mathrm{diag}[e^{i2\pi q_1}, e^{i2\pi q_2}, \ldots, e^{i2\pi q_N}], \tag{3.15}$$

by virtue of the parametrization of background $\bar{A}_4 = 2\pi/(g\beta)\mathrm{diag}(q_1, q_2, \ldots, q_N)$, with the real q_i satisfying the constraint $\sum_{i=1}^N q_i = 0$. As a phase factor, it is sufficient to work in the interval $0 \le q_i \le 1$. And now,

$$\hat{L}_A = \mathrm{diag}[1, 1, \ldots, 1, e^{i2\pi q_{ij}}, \ldots, e^{-i2\pi q_{ij}}], \tag{3.16}$$

where the $N-1$ "1" corresponds to the Cartan part, while the $N(N-1)/2$ pairs of $q_{ij} \equiv q_i - q_j$ with $N \ge i > j \ge 1$ corresponds to the non-Cartan part. The above form is more convenient and will be adopted hereafter. Then $1 - \hat{L}_A e^{-E_g/T} = \mathrm{diag}(1 - e^{-E_g/T}, \ldots, 1 - e^{i2\pi q_{ij} - E_g/T}, \ldots, 1 - e^{-i2\pi q_{ij} - E_g/T})$. We also define

$$\begin{aligned}\Omega(q_{ij}, M_g) &\equiv 2T \int \frac{d^3\vec{p}}{(2\pi)^2} \log(\det(1 - \hat{L}_A e^{-E_g/T})) \\ &= 2T \sum_{i,j=1}^N \left(1 - \frac{\delta_{ij}}{N}\right) \int \frac{d^3\vec{p}}{(2\pi)^3} \\ &\quad \times \log(1 - e^{-E_g/T} e^{2\pi i q_{ij}}),\end{aligned} \tag{3.17}$$

where in the second line we use $q_{ij} = -q_{ji}$ and allow $i = j$, to write the summation compactly.[4] In this notation, the gluonic part contribution to the effective potential $\mathcal{V}_{\mathrm{eff}}$ is $2\Omega(q_{ij}, M_g)$.

In the following, we present two important expansions of this potential, the low temperature and the high temperature expansion. Both will be used in the later discussions.

1. Low temperature expansion

In the QPM, it is found that the fitted $M_g(T)/T$ is sufficiently large at least around T_c, hence one has $E_g/T > M_g/T \gtrsim \mathcal{O}(1)$. We will find this is also true in our model from a full numerical study, which enables us to make a low temperature expansion for the effective potential around T_c. This leads to an analytical expression, which is useful in the phase transition analysis. First, we expand the logarithm in $\Omega(q_{ij}, M_g)$, retaining $\hat{L}_A$,

$$\Omega(\hat{L}_A, M_g) = -\frac{T}{\pi^2} \sum_{n=1}^\infty \frac{1}{n} \mathrm{tr}(\hat{L}_A)^n \int p^2 e^{-nE_g/T} dp. \tag{3.18}$$

Then we substitute $p = M_g \sinh t$ to get

$$\begin{aligned}\Omega(\hat{L}_A, M_g) &= -\frac{TM_g^3}{\pi^2} \sum_{n=1}^\infty \frac{1}{n} \mathrm{tr}(\hat{L}_A)^n \\ &\quad \times \int_0^\infty \cosh\, t \sinh^2 t e^{-n(M_g/T)\cosh t} dt\end{aligned} \tag{3.19}$$

Now we use the following trick to rewrite the integral as

$$\begin{aligned}\Omega(\hat{L}_A, M_g) &= \frac{T^2 M_g^3}{\pi^2} \sum_{n=1}^\infty \frac{1}{n^2} \mathrm{tr}(\hat{L}_A)^n \\ &\quad \times \frac{d}{dM_g} \int_0^\infty \sinh^2 t e^{-n(M_g/T)\cosh t} dt,\end{aligned} \tag{3.20}$$

[4] Actually, if we instead adopt the ladder basis for $su(N)$ and start from the eigenphase parametrization of $\bar{A}_4$ [17], the above expression can be explicitly obtained from the covariant derivative whose background dependent term reads $[\bar{A}_4, \hat{A}_\mu] \sim (q_i - q_j)\delta_{\mu 4}$.

where the integral can be done explicitly, $\sim K_1(x)$, and we finally arrive

$$\Omega(\hat{L}_A, M_g) = -\frac{T^2 M_g^2}{\pi^2}\sum_{n=1}^{\infty}\frac{1}{n^2}\mathrm{tr}(\hat{L}_A)^n K_2(nM_g/T). \quad (3.21)$$

with $K_i(x)$ the modified Bessel function of the second kind, of order i. For M_g/T moderately larger than 1, the leading order is a good approximation.

2. High temperature expansion

At the high temperature limit, where $1 \gg M_g/T$, one can find a simple analytic expression of $\Omega(q_{ij}, M_g)$; see also Ref. [49] for the complete high temperature expansions beyond the leading term. To that end, we again expand the logarithmic function:

$$\Omega(q_{ij}, M_g) = -\frac{T^4}{\pi^2}\sum_{i,j=1}^{N}\left(1-\frac{\delta_{ij}}{N}\right)\int_0^{\infty} dx x^2 \times \sum_{n=1}^{\infty}\frac{1}{n}e^{2\pi n i q_{ij}} e^{-\sqrt{n^2(x^2+\beta^2 M_g^2)}}. \quad (3.22)$$

Expand this expression according to βM_g, and we get

$$\Omega(q_{ij}, M_g) = -\frac{T^4}{\pi^2}\sum_{i,j=1}^{N}\left(1-\frac{\delta_{ij}}{N}\right)\int_0^{\infty} dx x^2 \times \sum_{n=1}^{\infty}\frac{1}{n}e^{2\pi n i q_{ij}}\left[e^{-nx} - \beta^2 M_g^2\frac{n e^{-nx}}{2x}\right] + \mathcal{O}(\beta^2 M_g^2). \quad (3.23)$$

The summation over n in the first term is straightforward, while in the second term, with one more "n" factor from the Taylor expansion, can be done as the following,

$$\sum_{n=1}^{\infty}\frac{1}{n}n e^{-nx} = -\left(\sum_{n=1}^{\infty}\frac{1}{n}e^{-nx}\right)' = -\frac{d}{dx}\log(1-e^{-x}). \quad (3.24)$$

Similar operations can be generalized to higher order of n, leading to higher derivative to $\log(1-e^{-x})$. Now, the first two terms are summed to

$$\Omega(q_{ij}, M_g) = -\frac{T^4}{\pi^2}\sum_{i,j=1}^{N}\left(1-\frac{\delta_{ij}}{N}\right) \times \int_0^{\infty} dx x^2 [\log(1-e^{-x+2\pi i q_{ij}}) + \frac{\beta^2 M_g^2}{2x}\frac{d}{dx}\log(1-e^{-x+2\pi i q_{ij}})]. \quad (3.25)$$

The result of these integration are just two Polylogarithm function

$$\Omega(q_{ij}, M_g) = -\frac{T^4}{\pi^2}\sum_{i,j=1}^{N}\left(1-\frac{\delta_{ij}}{N}\right) \times \left[2Li_4(e^{2\pi i q_{ij}}) - \frac{\beta^2 M_g^2}{2}Li_2(e^{2\pi i q_{ij}})\right] + \mathcal{O}(\beta^2 M_g^2). \quad (3.26)$$

Since $q_{ij} = q_i - q_j = -q_{ji}$ we can rewrite this expression into an analytic form by Jonquière's inversion formula

$$Li_n(e^{2\pi i x}) + (-1)^n Li_n(e^{-2\pi i x}) = -\frac{(2\pi i)^n}{n!}B_n(x), \quad (3.27)$$

where B_n is the Bernoulli polynomials. In our case, we can find that

$$Li_2(e^{2\pi i q_{ij}}) + Li_2(e^{2\pi i q_{ji}}) = 2\pi^2 B_2(q_{ij}),$$
$$Li_4(e^{2\pi i q_{ij}}) + Li_4(e^{2\pi i q_{ji}}) = -\frac{2\pi^4}{3}B_4(q_{ij}). \quad (3.28)$$

Substitute this formula into our expression to get

$$\Omega(q_{ij}, M_g) = \frac{1}{\pi^2}\sum_{i\geq j=1}^{N}\left(1-\frac{N-1}{N}\delta_{ij}\right) \times \left[\frac{4\pi^4}{3\beta^4}B_4(q_{ij}) + \frac{M_g^2\pi^2}{\beta^2}B_2(q_{ij})\right] + \mathcal{O}(\beta^2 M_g^2), \quad (3.29)$$

We can write it into a more simple form

$$\Omega(q_{ij}, M_g) = \frac{1}{\pi^2}\sum_{i,j=1}^{N}\left(1-\frac{\delta_{ij}}{N}\right) \times \left[\frac{2\pi^4}{3\beta^4}B_4(|q_{ij}|) + \frac{M_g^2\pi^2}{2\beta^2}B_2(|q_{ij}|)\right] + \mathcal{O}(\beta^2 M_g^2). \quad (3.30)$$

In the massless limit only B_4 is present.

C. The thermodynamic potential: Gauge-fixed part and phase transition

In this subsection, we include the contribution from the gauge-fixed part to the thermodynamic potential, and then study how first order deconfinement phase transition occurs due to the ghost contribution [35].

1. Infrared ghost domination

The ghost contribution is similar to that from the gluons because it is also in the adjoint representation. However, there are two key differences, which enable the contribution of the thermodynamic potential from the ghost fields to

successfully trigger the deconfinement phase transition. First, the ghost fields belong to Grassmann fields, and thus there is a minus sign relative to the gluon contribution. Second, the ghosts are still massless since the lattice data does not show that the correlators of ghost develop a massive pole. Moreover, we have to take into account the contribution from the gauge-fixing term. To deal with this term, we should do the quadratic partition between $\hat{A}^a$ and field h^a, to get two quadratic terms with the mixing term eliminated; the details can be found in Appendix A or in the textbook [50]. The final result of the total effective potential is given by

$$\mathcal{V}_{\text{eff}} = \frac{3}{2}\Omega(M_g) - \frac{1}{2}\Omega(M_g = 0), \tag{3.31}$$

The above result is in the Landau-DeWitt gauge, and as usual, the effective potential is gauge-dependent.

Without a quasigluon mass, the ghost contribution cancels the nonphysical gluonic contribution and then the potential fails to admit a phase transition. On the contrary, the presence of M_g makes the enhanced ghost contribution (relative to gluon contribution) dominate the potential at low temperature, realizing the inverted Weiss potential as the confining mechanism.

Because we are dealing with the phase transition where $T \to T_c$ and $M_g/T \gg 1$, it is fair for us to expand the first term by low temperature expansion Eq. (3.21). The second term is just the zero mass limit of Eq. (3.30) and thus high temperature expansion applies. Combining the above information, we can get the following analytic form of this effective potential

$$\begin{aligned}\mathcal{V}_{\text{eff}} &= 3T\int\frac{d^3\vec{p}}{(2\pi)^3}\text{tr}\log\left(1-\hat{L}_A e^{-\frac{E_g}{T}}\right)\\ &\quad - T\int\frac{d^3\vec{p}}{(2\pi)^3}\text{tr}\log\left(1-\hat{L}_A e^{-\frac{|\vec{p}|}{T}}\right)\\ &\simeq -\frac{3T^4}{2\pi^2}\left(\frac{M_g}{T}\right)^2 K_2(M_g/T)\text{tr}(\hat{L}_A)\\ &\quad -\frac{1}{2\pi^2}\sum_{i,j=1}^{N}\left(1-\frac{\delta_{ij}}{N}\right)\left[\frac{2\pi^4}{3\beta^4}B_4(q_{ij})\right].\end{aligned} \tag{3.32}$$

The first term can be translated to a function of PL, by using the identity $\text{tr}\hat{L}_A = \text{tr}\hat{L}_F\text{tr}\hat{L}_F^\dagger - 1$. Nevertheless, the ghost term contains $N-1$ independent variables q_i, rather than merely the trace part of $\hat{L}_F$. Hence, usually, one has to deal with a multidimensional field space, case by case.

A way to reduce the potential to the one-dimension problem is assuming the uniform eigenvalue distribution, i.e., $q_{ij} = \frac{i-j}{N}r$. It is automatically true for $N = 2, 3, 4$ with the number of independent eigenphases less than 4, but it is merely an ansatz for the even higher N. Such an ansatz has been adopted in Ref. [25], and is shown to work well. The ansatz is based on the observation that the confining vacuum, which is center symmetric, is characterized by the uniform eigenvalue distribution; dynamically, the distribution is a result of the eigenvalue repulse from the confining potential which involves the difference between eigenvalues q_i [25,51,52]. Furthermore, it is conjectured that the transition from the deconfining vacuum to the confining vacuum takes the shortest path, a straight line connecting the origin and the confining vacuum [25].[5] Then, we get the analytic potential for any color number

$$\begin{aligned}\mathcal{V}_{\text{eff}} &\simeq -\frac{3T^4N^2}{2\pi^2}\left(\frac{M_g}{T}\right)^2 K_2(M_g/T)l_N^2\\ &\quad -\frac{2\pi^2T^4}{3}\sum_{i=1}^{N}(N-i)B_4\left(\frac{i}{N}r\right)+f(N,T),\end{aligned} \tag{3.33}$$

where $f(N,T)$ is a function does not depend on the order parameter, only relevant to thermodynamics. We can easily carry out this summation and find that

$$\begin{aligned}\mathcal{V}_{\text{eff}} &\simeq -\frac{N^2}{2}\left(\frac{3T^4}{\pi^2}\left(\frac{M_g}{T}\right)^2 K_2(M_g/T)l_N(r)^2\right.\\ &\quad +\frac{\pi^2T^4}{45}\left[(-1+r)^2(-1-2r+2r^2)-\frac{5(-1+r)^2r^2}{N^2}\right.\\ &\quad \left.\left.+\frac{r^3(-4+3r)}{N^4}\right]\right)+f(N,T),\end{aligned} \tag{3.34}$$

which is somehow a hybrid of the PL model and matrix model.

Usually, $l_N = \text{tr}\hat{L}_F/N$ as a function of s is complicated. By definition, we can find that

$$l_N(r) = \begin{cases}\frac{1}{N}\left(1+2\sum_{i=1}^{\frac{N-1}{2}}\cos(2\pi\frac{i}{N}r)\right), & N \text{ is odd},\\ \frac{2}{N}\left(\sum_{i=1}^{\frac{N}{2}}\cos(2\pi\frac{2i-1}{2N}r)\right), & N \text{ is even}.\end{cases} \tag{3.35}$$

The summation can be implemented by writing $\cos(nx) = \text{Re}\exp(inx)$, translating it to the geometric series, and then we obtain the simple expression

$$l_N(r) = \frac{1}{N}\frac{\sin(\pi r)}{\sin(\pi r/N)}, \tag{3.36}$$

[5]This is not the very precise statement. At high T, the origin namely $A_0 = 0$ is the deconfining vacuum. As T decreases to near T_c, it moves away from the origin to the configuration still characterized by the uniform eigenvalue distribution. In the effective matrix model, this is shown to be a good approximation even for the relatively small N [25].

which holds both for odd and even N. In particular, when the color number approaching infinity, PL takes the limit $\sin(\pi r)/(\pi r)$.

2. Deconfinement phase transition

Now we arrive the effective potential which can be used to study deconfinement phase transition for any color number N. For a sufficiently large N, one can simply use the following rescaled potential

$$\frac{\mathcal{V}_N(r,T)}{N^2/2} \simeq -\frac{3T^4}{\pi^2}\left(\frac{M_g}{T}\right)^2 K_2(M_g/T)\left[\frac{\sin(\pi r)}{\pi r}\right]^2 + \frac{\pi^2 T^4}{45}(r-1)^2(1+2r-2r^2), \tag{3.37}$$

which is N-independent. To find the vacuum position of this potential, one should calculate the derivative of this potential with respect to r, to solve the following tadpole equation

$$\frac{6}{\pi^2}\left(\frac{M_g}{T}\right)^2 K_2(M_g/T)\frac{\pi\sin(\pi r)(\cos(\pi r)-\frac{1}{N}\sin(\pi r)\cot(\frac{\pi r}{N}))}{N^2\sin^2(\pi r/N)} + \frac{\pi^2}{45}r(r-1)\left[2(4r-5)-\frac{10}{N^2}(2r-1)+\frac{12}{N^4}r\right]=0. \tag{3.38}$$

It has two obvious solutions: (1) $r=0$, the deconfined vacuum position at high temperature; (2) $r=1$, the confining vacuum position, which is consistent with the Z_N symmetry argument: The confining vacuum should preserve the Z_N symmetry and then the PL value must be $l_N(r=1)=0$. In our model, this is trivially satisfied for the potential from gluons, which contributes the quadratic term l_N^2. However, the inverted Weiss term is not a polynomial of l_N, and therefore $r=1$ (namely $l_N=0$) being its extremum is nontrivial. It is attributed to the eigenvalue repulse of the potential. Equation (3.38) may also admit solutions for $r\neq 1$, the candidates for the deconfined vacuum at the lower temperature.

For a given N, the shape of the potential Eq. (3.34) is solely determined by the single dimensionless parameter $M_g(T)/T$. Then, we plot the shape function $\mathcal{U}_N \equiv \mathcal{V}_N(r,T)/N^2$ at different values of $M_g(T)/T$, to search the vacuum structure; the plots are displayed in Fig. 1. For the $N=2$ case, there is only one minimum at $s\neq 1$, and eventually, only the minimum at $s=1$ survives as the increasing $M_g(T)/T$; see the left panel of Fig. 1. So, in this case, the transition from the deconfined phase to the confining phase is crossover. On the contrary, for the case $N\geq 3$, $\mathcal{U}_N$ has two minimums when $M_g(T)/T$ approaches 2.7, with one located at $r=1$ and the other one at $r\neq 1$. It implies that the deconfinement phase transition is first order. Furthermore, via the degeneracy condition, we can determine the critical temperature T_c in the unit of $M_g(T_c)$; see the right panel of Fig. 1.

The phase transition behavior predicted by the model is consistent with the results of lattice simulation. Hence, it is of importance to understand what causes the qualitative difference between the shape functions for $N=2$ and $N\geq 3$. To that end, we investigate the shape function near $r=1$, and hence it is convenient to set $t=1-r$; then, we expand it around $t=0$,keeping the irrelevant terms up to $\mathcal{O}(t^5)$,

$$\mathcal{U}_N = t^2\left(\frac{\pi^2 c_g \csc^2\frac{\pi}{N}}{N^2}+\frac{6}{N^4}-\frac{5}{N^2}-1\right) + t^3\left(\frac{2\pi^3 c_g \cot\frac{\pi}{N}\csc^2\frac{\pi}{N}}{N^3}-\frac{8}{N^4}+\frac{10}{N^2}-2\right) + t^4\left[c_g\frac{\pi^4\csc^2\frac{\pi}{N}}{3N^2}\left(\frac{3}{N^2}+\frac{9\cot^2\frac{\pi}{N}}{N^2}-1\right)+\frac{3}{N^4}-\frac{5}{N^2}+2\right], \tag{3.39}$$

where $c_g \equiv (M_g/T)^2 K_2(M_g/T)$. The special property of $N=2$ case is that the cubic term vanishes and therefore

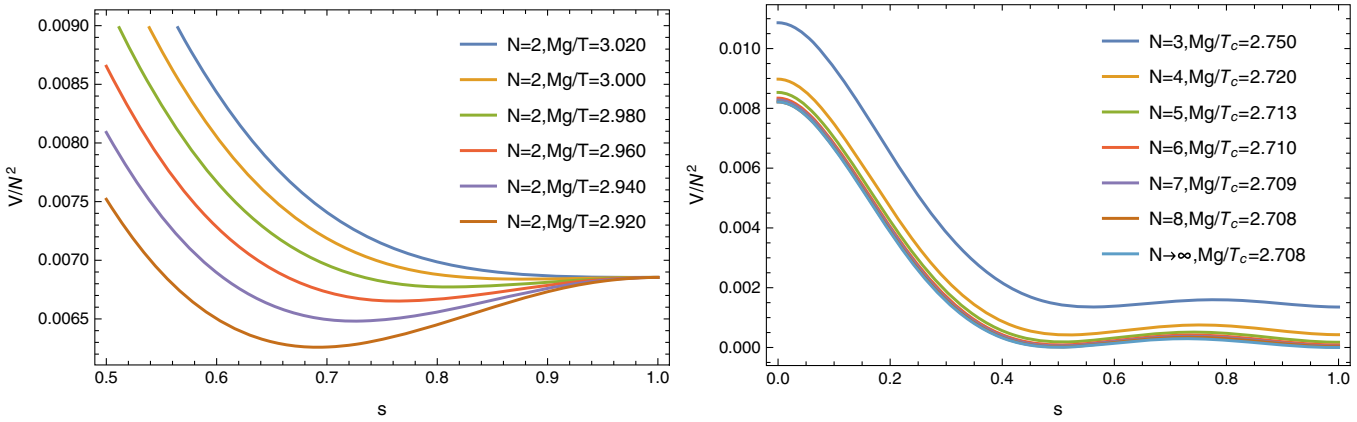

FIG. 1. Left panel: The potential behavior for $SU(2)$ theory around the critical temperature. Right panel: The potential shape for $SU(N\geq 3)$ at the critical temperature.

there is no barrier. For $N > 2$, the cubic term is present and moreover carries a positive coefficient (attributed to the gluon potential), and as a consequence $\mathcal{U}_N$ is able to give rise to the first order deconfinement phase transition.

We end up this section with a comment on the Haar-type model [18–21], whose potential is supposed to resemble

$$V = -a(T)l^2/2 + b(T)\log H_N(L). \tag{3.40}$$

The first term of this potential comes from the kinetic term of $SU(N)$ theory which also exists in our model. The second term, characterized by $H_N(L)$, actually is known as the Vandermonde determinant interaction of the $SU(N)$ theory; it appears mathematically to define an integration over a continuous group, which requires an invariant Haar group measure. Such an interaction is non perturbative, and is argued to be consistent with the picture of ghost dominance. Explicitly, the integrand functional of our effective potential $-\Omega(M_g = 0)$ in the infrared regime $(E, p \to 0)$ resembles the Vandermonde determinant interaction. In other words, roughly speaking it is a part of the ghost contribution.

IV. THERMODYNAMICS

Although the model can surprisingly describe the order of deconfinement phase transition for any N, it is still important to check if it is able to correctly account for the thermodynamics above T_c, in particular in the semi-QGP region around $1.4T_c$ where the nonperturbative effect is significant. We have to rely on the temperature varying $M_g(T)$, with $M_g(T_c)$ fixed (traded with the critical temperature T_c), to do this job.

We should start from fitting latent heat. Because the quasi gluon mass is temperature dependent, the latent heat is sensitive to dM_g/dT at T_c. Actually, the latent heat data can fix the value of this derivative at T_c, which is crucial to fit $M_g(T)$ via thermodynamics.

A. Latent heat and determination of $dM_g(T)/dT$ at T_c

From the thermodynamics, it is known that the latent heat L_N released during the first order phase transition is the energy density difference between two vacua, $L_N = \varepsilon_d - \varepsilon_c$, with subscripts d and c denoting for the deconfined and confining vacuum, respectively. Then, using the second law of thermodynamics, one can find that

$$L_N = T_c\frac{\partial \Delta P}{\partial T} - \Delta P = -T_c\frac{\partial \Delta \mathcal{V}(T)}{\partial T}\bigg|_{T=T_c} + \Delta\mathcal{V}_N(T_c), \tag{4.1}$$

where $\Delta\mathcal{V}_N = \mathcal{V}_d - \mathcal{V}_c$ is the potential energy difference, vanishing at T_c. As a consequence, the latent heat is determined by the entropy part, i.e., $L_N = -T_c\frac{\partial\Delta\mathcal{V}(T)}{\partial T}|_{T=T_c}$.

Note that so far we cannot guarantee the confining vacuum at $s = 1$ is indeed the absolute minimum below T_c, but it is simply an inference of the requirement that latent heat should be positive: It means $\partial\mathcal{V}_d/\partial T_c < \partial\mathcal{V}_c/\partial T_c$, and moreover at T_c two vacua is degenerate, $\mathcal{V}_d = \mathcal{V}_c$, so, below T_c one indeed has $\mathcal{V}_d < \mathcal{V}_c$.

We are now in the position to calculate the latent heat in our model. The straightforward calculation of the temperature derivative of the effective potential gives

$$\begin{aligned}\frac{\partial\mathcal{V}(r,T)}{\partial T} = &-\frac{3M_g^2N^2}{2\pi^2}l_N^2\bigg[4TK_2(M_g/T)\\ &+K_1(M_g/T)\left(M_g - T\frac{dM_g}{dT}\right)\bigg]\\ &-N^2\frac{2\pi^2}{45}\bigg[(-1+r)^2(-1-2r+2r^2)\\ &-\frac{5(-1+r)^2r^2}{N^2}+\frac{r^3(-4+3r)}{N^4}\bigg]T^3,\end{aligned} \tag{4.2}$$

In our model, the confining vacuum is always located at $r = 1$ or $l_N = 0$, and thus the contribution of the above derivative in this vacuum is a trivial term. Then, the latent heat is determined by the contribution from the deconfined vacuum,

$$\begin{aligned}\frac{L_N}{(N^2-1)T_c^4} = &\frac{N^2}{N^2-1}\left(\frac{3l_{N,d}^2}{2\pi^2}\left(\frac{M_g}{T_c}\right)^2\bigg[4K_2(M_g/T_c)\right.\\ &\left.+K_1(M_g/T_c)\left(\frac{M_g}{T_c}-\frac{dM_g}{dT_c}\right)\bigg]\right.\\ &+\frac{2\pi^2}{45}\bigg[\left(-1+r_d\right)^2(-1-2r_d+2s_d^2)\\ &-\frac{5(-1+r_d)^2r_d^2}{N^2}+\frac{r_d^3(-4+3r_d)+1}{N^4}\bigg]\bigg),\end{aligned} \tag{4.3}$$

where r_d (or $l_{N,d}$) is the value of r (or l_N) in the deconfined vacuum, numerically calculated by virtue of the tadpole Eq. (3.38), shown in Table I.

TABLE I. Effective mass, the position of deconfined vacuum and, latent heat around the critical temperature for different color number N.

Color number	$N=3$	$N=4$	$N=5$	$N=6$	$N=7$	$N=8$	$N\to\infty$
r_d	0.5605	0.5186	0.5073	0.5033	0.5016	0.5009	0.5004
l_d	0.5910	0.6300	0.6380	0.6398	0.6400	0.6396	0.6367
$M_g(T_c)/T_c$	2.7499	2.7203	2.7126	2.7099	2.7088	2.7083	2.7077
$dM_g(T_c)/dT_c$	−5.7727	−7.9951	−9.2891	−10.0965	−10.6261	−10.9954	−12.3376
$L_N/(N^2-1)T_c^4$	0.2091	0.2874	0.3236	0.3433	0.3551	0.3628	0.3880

On the other hand, for $N = 3, \ldots 8$, the current lattice data gives the following behavior of latent heat [53]

$$\frac{L_N}{(N^2-1)T_c^4} \simeq 0.388 - \frac{1.61}{N^2}, \tag{4.4}$$

We require the calculated latent heat Eq. (4.3) to fit it. For the given N, Eq. (4.3) just contains a single parameter, $dM_g(T)/dT$ at T_c, and therefore its value can be uniquely fixed. We show the results in Table I. The resulting values typically are around -10 for all N, indicating a sharp increasing of quasi-gluon mass as the temperature drops down to T_c from above. This is a well-understood behavior since it can be regarded as a sign of the "strongest" nonperturbative effect near T_c.

B. Fit M_g with the thermal quantity using machine learning

According to the original idea of QPM, the proper temperature dependence beyond T_c of quasigluon mass is supposed to successfully explain the thermodynamics of the hot PYM system up to the high T region. Here, the main thermodynamic observables of interest are the pressure p, the energy density ϵ, and the entropy density s. Actually, they are not independent quantities. In particular,

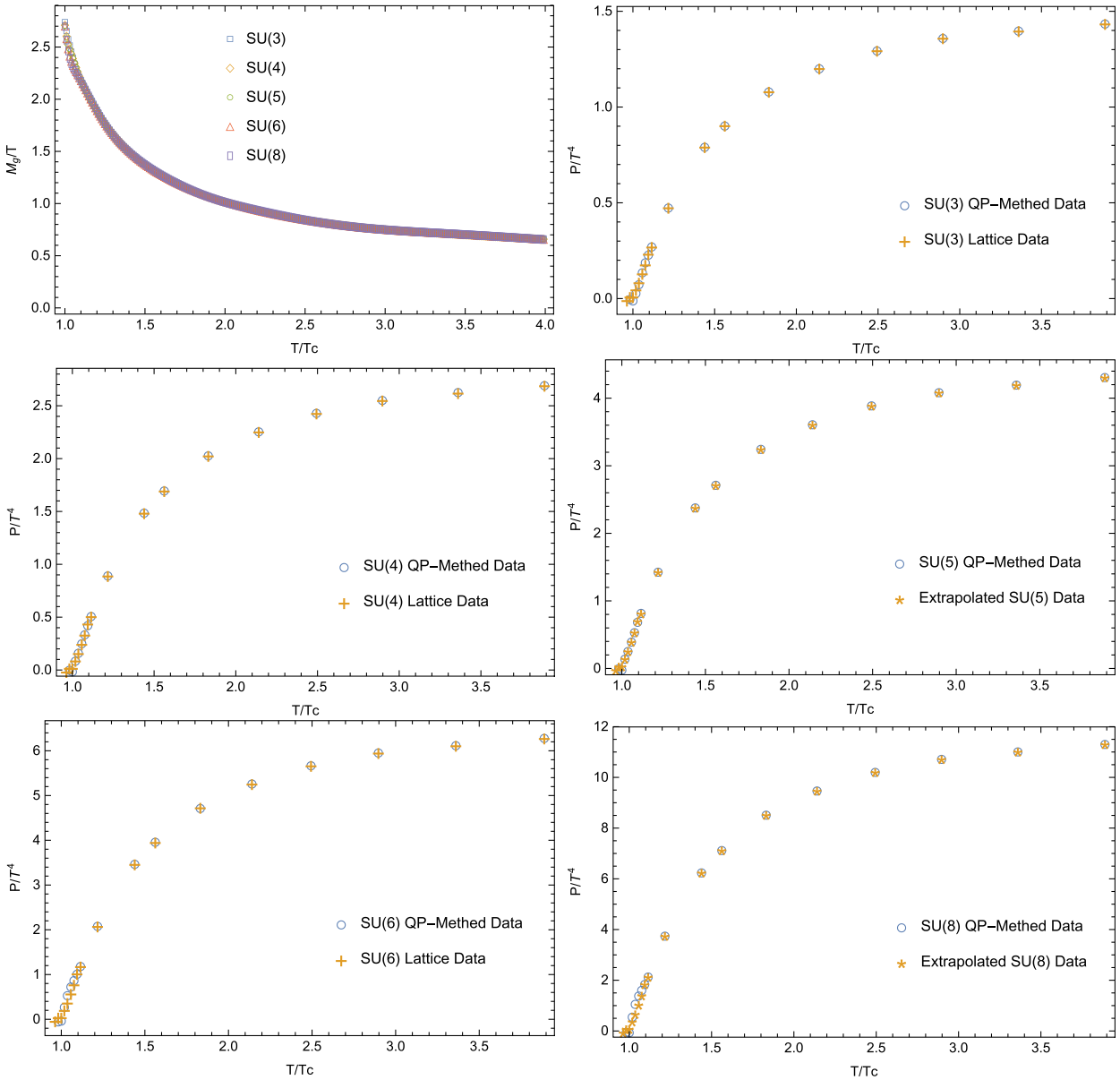

FIG. 2. The first panel: The fitted M_g/T as a function of temperature for $N = 3, 4, 5, 6, 8$. The second to the sixth panels: Fitting p/T^4 in our model for various color number.

if one has p, then ϵ and s can be calculated by the second law of thermodynamics

$$\epsilon = T\frac{dp}{dT} - p, \qquad s = \frac{\epsilon + p}{T}. \tag{4.5}$$

The one loop calculation leads to $p = -\mathcal{V}_{\text{eff}}$, given in Eq. (3.34). Currently, their lattice data is available only for $N = 3, 4, 6$ [53]. However, as stated in the introduction, the lattice data demonstrates N scaling property, which means $P_M = \frac{M^2-1}{N^2-1}P_N$ and the latent Eq. (4.4), and thus we also have "data" for other N values by simple extrapolation, for instance to $N = 5$, 8 used later.

In the QPM, it is known that the SB limit can be trivially recovered. The most challenging range is the so-called semi-QGP region $T \in (T_c, 3T_c)$, where the deviation to the blackbody behavior becomes more and more remarkable as T approaching T_c. In the previous discussion, we have used effective potential Eq. (3.32), which is based on the high and low temperature expansion, to analyze the phase

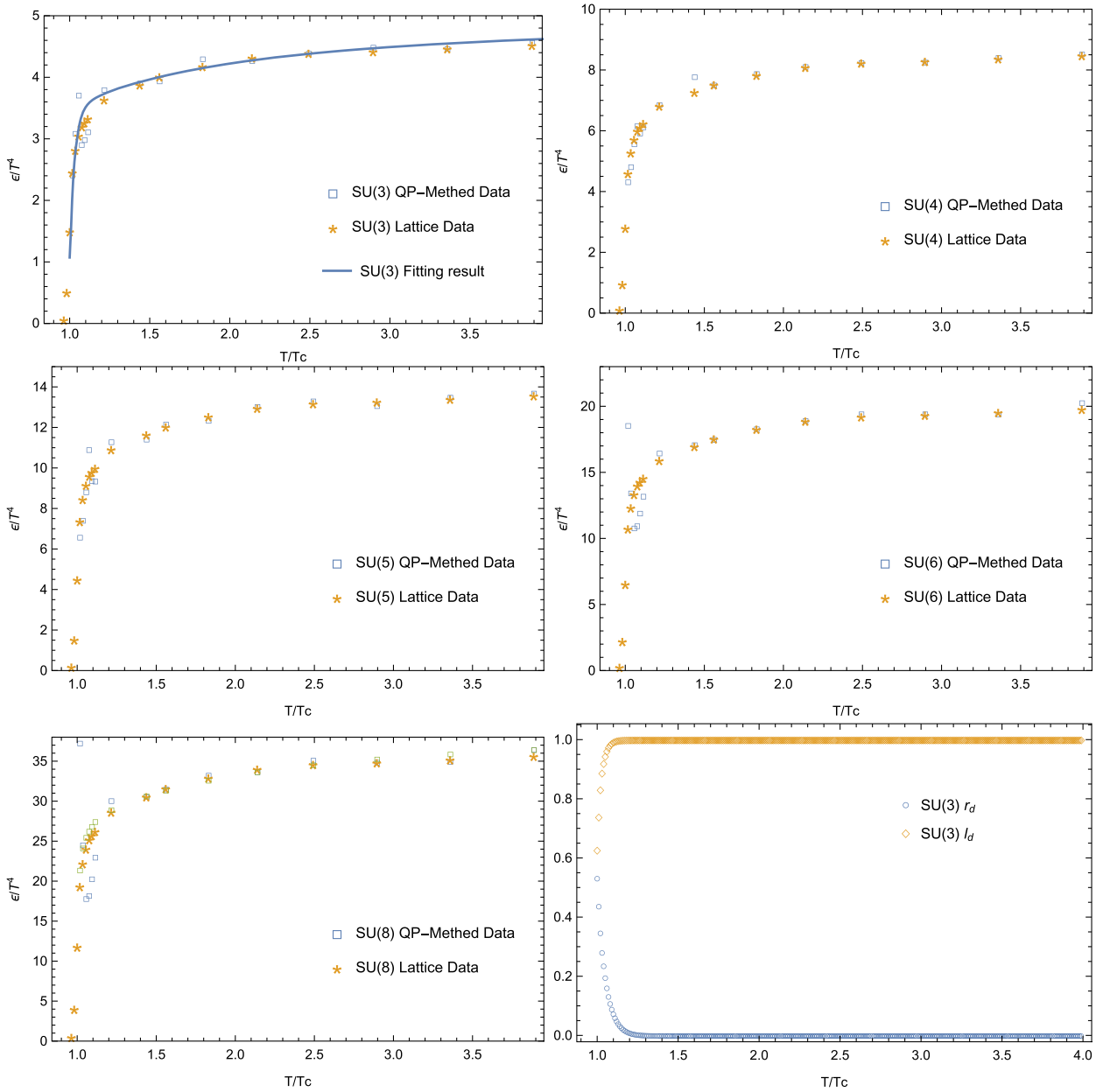

FIG. 3. From the first to the fifth panels: energy density for $N = 3, 4, 5, 6, 8$ (the blue square denoting for model prediction using the numerical function M_g from machine learning; the yellow star denoting for lattice data; in the first panel, for comparison, the prediction using the smooth fitting function Eq. (4.9) for M_g labeled as the blue line). The last panel: the value of the order parameter in the deconfinement phase l_d (or r_d) varying with temperature for $N = 3$.

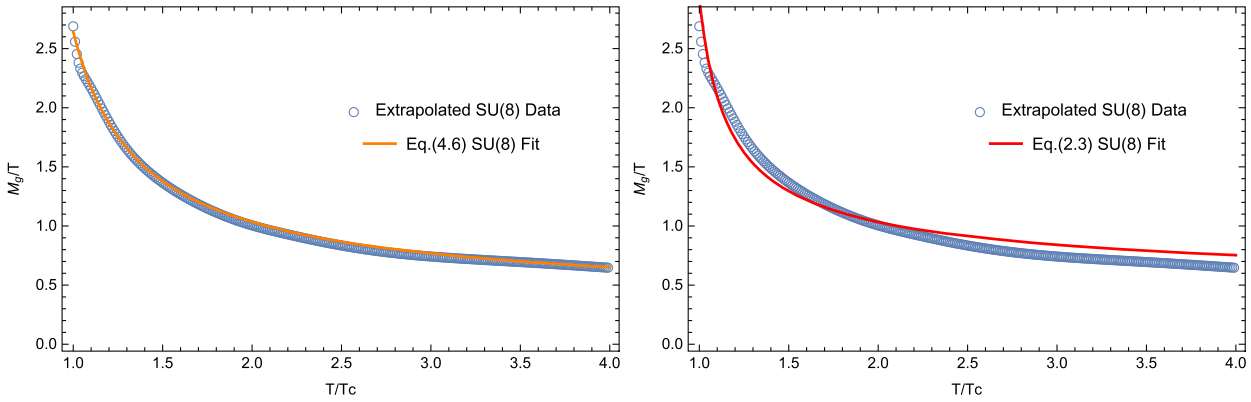

FIG. 4. The fitting for the quasigluon mass ansatz Eqs. (4.9) (left panel) and (2.3) (right panel), where the fitting parameters are given in Table II.

transition at T_c. Nevertheless, we do not have such a simple analytic expression to analyze thermodynamics. It is well expected that the low temperature expansion just holds very near T_c and soon becomes not reliable in the higher temperature region. Hence, we should use its complete expression:

$$\mathcal{V}_{\text{eff}} = \frac{T^4}{2\pi^2}\int_0^\infty dx x^2 \Bigg((N-1)\log[1-e^{-\hat{E}(x,M_g,T)}] + \sum_{i=1}^{N}(N-i)\log\Bigg[1+e^{-2\hat{E}(x,M_g,T)} - 2e^{-\hat{E}(x,M_g,T)}\cos\left(2\pi\frac{ir}{N}\right)\Bigg]\Bigg) + \cdots, \tag{4.6}$$

where $\hat{E}(x,M_g,T) = \sqrt{x^2+(M_g/T)^2}$ and dots denote for the remaining term that does not need summation.

Then, we try to obtain the interpolation function of the fitted effective gluon mass $M_g(T)$ for $N = 3, 4, 5, 6, 8$, through the method of machine learning. Physical information neural network [54] provides us with a flexible and accurate method for the fitting task. It treats functions of any complexity under fitting as a neural network, and the training goal is making the neural network satisfying the required partial differential relationships (such as partial differential equations and boundary conditions) and the given data points values. In our work, we use two separate deep neural networks $M_g(T)$ and $r(T)$ for the fitting task, and our training goal is making $M_g(T)$ and $r(T)$ to satisfy:

(i) the extreme condition for the deconfined vacuum,

$$\left.\frac{\partial\mathcal{V}(r,T,N)}{\partial r}\right|_{r=r_d(T)} = 0; \tag{4.7}$$

(ii) the degeneracy between the deconfined vacuum and the confining vacuum,

$$\mathcal{V}(r,T,N)|_{r=r_d(T=T_c),T=T_c} = \mathcal{V}(1,T_c,N); \tag{4.8}$$

(iii) mass parameter relationship in Table I and

(iv) the lattice data for thermodynamics.

We implement the task using TensorFlow2.0 [55], both $M_g(T)$ and $r(T)$ containing 7 hidden layers, each of which includes 64, 128, 256, 512, 256, 128, 64 neutrons respectively. For the complexity of our problem, we should adopt a two-step training: We pretrain $M_g(T)$ and $r(T)$ to fit the lattice data first, and then fine adjust $M_g(T)$ and $r(T)$ to satisfy other fitting requirements. Such a procedure motivates us to divide the training samples into two types, the first type satisfies the lattice thermodynamic data at T_c, and the second type is 128 points randomly distributing in the temperature region $[T_c, 4T_c]$, which meet the other three theoretical conditions listed above. For more details, please check the code in Github.[6] The fitted $M_g(T)$ is shown in the first panel of Fig. 2, and the perfect fitting of pressure above T_c is displayed in other panels of Fig. 2.

With the fitted $M_g(T)$, one can plot the energy density ϵ, shown in Fig. 3. From the first five plots one can see that our model predictions fairly well match the lattice data for all N, except that the point around $1.3T_c$ always mildly deviates from the lattice result. The reason is that our training did not include energy density data, and the resulting numerical function $M_g(T)$ is continuous but its derivative is discontinuous (retraining may lead to slight improvement). However, if we instead use the smooth fitting function Eq. (4.9) obtained later rather than the original numerical function, the calculated energy density can fit well with the lattice data, as shown in the example of $SU(3)$ in Fig. 3.

We also plot the value of the order parameter in the deconfinement phase, the Polyakov loop l_d or equivalently r_d here. We only show the $SU(3)$ case in the last panel of Fig. 3, which has been studied on the lattice; from the plot we can see that as the temperature rises, the value of l_d/r_d soon approaches $1/0$. The overall trend is right, but the $l_d(T)$ predicted in our model reaches 1 faster than the lattice result. This issue might be resolved by considering the

[6] https://github.com/JGuoHep/QuasiParticle.

TABLE II. α, β and γ are fitting parameters in the quasigluon mass ansatz Eq. (4.9), while λ and T_s are fitting parameters in the conventional ansatz Eq. (2.3).

α	β	γ	RMSD
0.029534	1.130884	1.541299	0.015707
0	1.186505	1.570699	0.016224

Void	λ	T_s	RMSD
Void	10.843298	−8.336149	0.081482

dressing propagators, which introduce more parameters; for comparison, here we have only one parameter, M_g. We leave this study to the future work.

The $M_g(T)$ is supposed to depend on N: Although $M_g(T_c)/T_c$ is almost universal determined by the condition of degeneracy, $dM_g(T)/dT$ takes different values at T_c for different color number for the sake of correct latent heat, see Table I. However, it is found that the fitted $M_g(T)$ are almost the same, which leads us to conjecture that this is an universal behavior for all N.[7] By the way, one can check the invalidation of low temperature expansion in the region $T \gtrsim 1.4T_c$: The ratio M_g/T drops to ≈ 1.5 as T increases to $1.4T_c$, and then from Eq. (3.21) one can see that the next leading order is only suppressed by a factor $K_2(2\times 1.5)/K_2(1.5) \sim 0.1$.

Actually, the N universal behavior of quasigluon mass is encoded in the quasigluon mass in the HTLpt; see the formula Eq. (2.3) where N cancels. At this point, our model is consistent with the HTLpt effective mass. So, it is anticipated that the interpolation function can be fitted by the $M_g(T)$ with the function given in Eq. (2.3), with two parameters λ and T_s. We also try another function with three parameters

$$M_g(T) = \alpha T + \beta T/\log(\gamma T/T_c). \tag{4.9}$$

which is recently adopted in Ref. [33]. Note that unlike the conventional $M_g(T)$ ansatz, which simply goes to the HTLpt quasigluon mass in the high T region, Eq. (4.9) does not. The fitted parameters for both functions of $M_g(T)$ are shown in Table II. The latter has better quality, which can be seen from the comparison in two panels of Fig. 4. This may raise the issue of well consistence between our model with the HTLpt in the higher T region, and we will come back to this point in the section of Conclusion and Discussion. Besides, for the function Eq. (4.9), from Table II one can see that the values of the α parameter are far smaller than the other two parameters, which means that it is almost irrelevant to fitting. So, we tried the fitting with the vanishing α, to find that it works equally well.

[7]For large N this is trivial, because the N dependence of the observables in our model is scaled out, well consistent with the lattice data. But it is not trivial that it is true also for $N = 3, 4$. By contrast, in the polynomial model [1], the fitting parameters in the small N cases are very different than those in the large N cases. We guess it is attributed to the exponential dependence of the fitting parameter $M_g(T)$.

V. CONCLUSION AND DISCUSSION

The HTL resummation in the quasi-particle picture reveals that QGP is a pool of weakly interacting quasigluons for $T \gtrsim 2T_c$. Such a picture is further used in the QPM to describe QCD thermodynamics down to T_c and works fairly well. The crucial idea is that the quasigluon mass could "absorb" strong interaction and merely leaves weak interactions on quasigluons. In this work we attempt to embed this idea to the massive PYM [35], introducing a temperature-dependent quasigluon mass in the effective $SU(N)$ PYM Lagrangian Eq. (3.2). Via the standard perturbative calculation, we obtain an effective model that can successfully explain the critical behavior for any N, not also the first order deconfinement phase transition for $N > 2$ but also the crossover for $N = 2$. Moreover, the lattice data of thermodynamics can be fitted via the single parameter $M_g(T)$, which is found to demonstrate the N-universal behavior, based on the available case $N = 3$, 4, 6. This is supported by the HTLpt quasigluon mass, but now is extended to the semi-QGP region, and might convey some secrets of the nonperturbative effects. We look forward to the future lattice data for other N, in particular, $N = 5$, 8 whose "lattice data" is obtained by extrapolation via the N-scaling law, to test the universal quasigluon mass conjecture.

Fitting $M_g(T)$ via a function that well matches with the HTLpt quasigluon mass does not have a very good quality, and it may be improved by considering the dressing propagator of the gluons [56]. Then, the modified model contains more parameter and have the potential to deal with more detailed problems.

We are capable of conducting a unified analysis of all N, depending on the assumption of uniform eigenvalue distribution of the temporal background, which reduces the effective potential to the one-dimensional case. But it is based on the eigenvalue repulsion and a more solid argument may be necessary.

ACKNOWLEDGMENTS

This work is supported in part by the National Key Research and Development Program of China Grant No. 2020YFC2201504 and in part by the National Science Foundation of China (11775086).

Note added.—Right before the submission of this work, the work by Fu-Peng Li etc. [57] appeared on arxiv. They also utilize the machine learning to reconstruct QCD equation of state in the QPM picture, which may have partial overlap with our work.

APPENDIX A: DERIVATION OF THE GENERATING FUNCTION IN THE LANDAU-DEWITT GAUGE

The complete Faddeev-Popov Lagrangian in the Landau-DeWitt gauge reads

$$\mathcal{L} = -\frac{1}{2g^2}\mathrm{tr}(F_{\mu\nu}F^{\mu\nu}) + \bar{D}_\mu \bar{c}^a D^\mu c^a + ih^a \bar{D}_\mu \hat{A}^{\mu,a} + \frac{1}{2}M_g(T)A^a_{tr,\mu}A^{a,\mu}_{tr}, \tag{A1}$$

We are considering the constant background $\bar{A}^a_\mu = \bar{A}^a_0\delta_{\mu 0}$ and keep only the quadratic terms. Then the action can be split into two parts $S_{A,h}$ and S_c, where

$$S_{A,h} = \int d^4x\left[\frac{1}{2}\hat{A}^a_\mu (D^{-1})_{ab}\hat{A}^{\mu,b} + ih^a\bar{D}_\mu\hat{A}^{\mu,a}\right]$$
$$S_c = \int d^4x[\bar{D}_\mu\bar{c}^a\bar{D}^\mu c^a], \tag{A2}$$

where D^{-1} is given in Eq. (3.6).

Now we come to deal with the first part of the action. We can rewrite this action in its color diagonalization basis $\tilde{A}^a_\mu$ and $\tilde{h}^a$, to get

$$S_{A,h} = \int d^4x\left[\frac{1}{2}\tilde{A}^a_\mu(\tilde{D}^{-1})_a\tilde{A}^{\mu,a} + i\tilde{h}^a\tilde{D}^a_\mu\tilde{A}^{\mu,a}\right] = \int \frac{d^4p}{(2\pi)^4}\left[\frac{1}{2}\tilde{A}^a_\mu(\tilde{D}^{-1})_a\tilde{A}^{\mu,a} + i\tilde{h}^a\tilde{D}^a_\mu\tilde{A}^{\mu,a}\right], \tag{A3}$$

where $(\tilde{D}^{-1})_a$ and $\tilde{D}^a_\mu$ in the momentum space are respectively given by

$$\tilde{D}^{-1}_a(p) \equiv D(M_g)^{-1}_a = (p_0 - A_a)^2 + |\vec{p}|^2 + M_g^2,$$
$$\tilde{D}^a_\mu\tilde{D}^{\mu,a} \equiv D(0)^{-1}_a = (p_0 - A_a)^2 + |\vec{p}|^2. \tag{A4}$$

To integrate this action through path integration, we must do the quadratic partition between $\tilde{A}^a$ and $\tilde{h}^a$. After a tedious quadratic partition, the action takes the form of

$$S_{A,h} = \int \frac{d^4p}{(2\pi)^4}\frac{1}{2}\left[(\tilde{D}^{-1})_a\left(\tilde{A}^a_\mu + i\frac{\tilde{D}^a_\mu}{\tilde{D}^{-1}_a}\tilde{h}^a\right)\times\left(\tilde{A}^{\mu,a} + i\frac{\tilde{D}^{\mu,a}}{\tilde{D}^{-1}_a}\tilde{h}^a\right) + \frac{\tilde{D}^a_\mu\tilde{D}^{\mu,a}}{\tilde{D}^{-1}_a}\tilde{h}^a\tilde{h}^a\right]. \tag{A5}$$

Now define a new field $\mathcal{A}^a_\mu = \tilde{A}^a_\mu + i\frac{\tilde{D}^a_\mu}{\tilde{D}^{-1}_a}\tilde{h}^a$, and one can rewrite the original mixed action as

$$S_{A,h} = \int \frac{d^4p}{(2\pi)^4}\frac{1}{2}\left[\mathcal{A}^a_\mu D(M_g)^{-1}_a\mathcal{A}^{\mu,a} + \frac{D(0)^{-1}_a}{D(M_g)^{-1}_a}\tilde{h}^a\tilde{h}^a\right]. \tag{A6}$$

The redefined Nakanishi-Lautrup field $\tilde{h}^a$ now gains a mass, and its propagator is a combination of the massive and massless propagators, which is a result of the Landau-Dewitt gauge. Then the 1-loop effective action is given by

$$\log Z_{A,h} = \frac{1}{2}\log\det\left[\frac{\delta^2 S_{h,A}}{\delta\phi^a_i\phi^a_j}\right] = 2\log\det(D(M_g)^{-1}) - \frac{1}{2}\log\det(D(M_g)^{-1}) + \frac{1}{2}\log\det(D(0)^{-1}) = \frac{3}{2}\log\det(D(M_g)^{-1}) + \frac{1}{2}\log\det(D(0)^{-1}). \tag{A7}$$

where ϕ^a_i represent $\{\mathcal{A}^a_\mu, \tilde{h}^a\}$. Note that there is a overall factor 4 for the $\mathcal{A}^a_\mu$ contribution, denoting for four massive modes. But the Nakanishi-Lautrup field cancels one massive mode and effectively just leaves one massless mode.

The massless ghost contribution, taking into account its statistics, is simply given by

$$\log Z_c = -\log\det(D(0)^{-1}). \tag{A8}$$

Its contribution is halved due to the massless mode of the Nakanishi-Lautrup field. Finally, the total effective action is

$$\log Z = \frac{3}{2}\log\det(D(M_g)^{-1}) - \frac{1}{2}\log\det(D(0)^{-1}). \tag{A9}$$

APPENDIX B: CALCULATING THE PURE GLUONIC GENERATING FUNCTION: THE $SU(4)$ SAMPLE

In this appendix we present the details of calculating the pure glunoic part, i.e., the first term of the second line of Eq. (A7), specified to $SU(4)$. Its Cartan generators are

$$T^3 = \frac{1}{2}\begin{pmatrix}1&0&0&0\\0&-1&0&0\\0&0&0&0\\0&0&0&0\end{pmatrix},\quad T^8 = \frac{1}{2\sqrt{3}}\begin{pmatrix}1&0&0&0\\0&1&0&0\\0&0&-2&0\\0&0&0&0\end{pmatrix},$$
$$T^{15} = \frac{1}{2\sqrt{6}}\begin{pmatrix}1&0&0&0\\0&1&0&0\\0&0&1&0\\0&0&0&-3\end{pmatrix}. \tag{B1}$$

Now the propagators take the form of (the quasigluon mass can be trivially included)

$$(D^{-1})_{ab} = \delta_{ab}p^2 + 2i\sum_{i=3,8,15} f_{abi}\bar{A}^i_0 p_0 - \sum_{i,j=3,8,15} f_{aci}f_{cbj}\bar{A}^i_0\bar{A}^j_0. \tag{B2}$$

After a careful calculation, one can get all the nonzero propagators

$$
\begin{aligned}
&(D^{-1})_{1,1} = p^2 + (\bar{A}_0^3)^2 \qquad (D^{-1})_{1,2} = 2ip_0\bar{A}_0^3\\
&(D^{-1})_{2,2} = p^2 + (\bar{A}_0^3)^2 \qquad (D^{-1})_{1,2} = -2ip_0\bar{A}_0^3\\
&(D^{-1})_{3,3} = p^2\\
&(D^{-1})_{4,4} = p^2 + \frac{1}{4}(\bar{A}_0^3)^2 + \frac{4}{3}(\bar{A}_0^8)^2 + \frac{\sqrt{3}}{2}\bar{A}_0^3\bar{A}_0^8 \qquad (D^{-1})_{4,5} = ip_0\bar{A}_0^3 + \sqrt{3}ip_0\bar{A}_0^8\\
&(D^{-1})_{5,5} = p^2 + \frac{1}{4}(\bar{A}_0^3)^2 + \frac{4}{3}(\bar{A}_0^8)^2 + \frac{\sqrt{3}}{2}\bar{A}_0^3\bar{A}_0^8 \qquad (D^{-1})_{5,4} = -ip_0\bar{A}_0^3 - \sqrt{3}ip_0\bar{A}_0^8\\
&(D^{-1})_{6,6} = p^2 + \frac{1}{4}(\bar{A}_0^3)^2 + \frac{4}{3}(\bar{A}_0^8)^2 - \frac{\sqrt{3}}{2}\bar{A}_0^3\bar{A}_0^8 \qquad (D^{-1})_{6,7} = -ip_0\bar{A}_0^3 + \sqrt{3}ip_0\bar{A}_0^8\\
&(D^{-1})_{7,7} = p^2 + \frac{1}{4}(\bar{A}_0^3)^2 + \frac{4}{3}(\bar{A}_0^8)^2 - \frac{\sqrt{3}}{2}\bar{A}_0^3\bar{A}_0^8 \qquad (D^{-1})_{7,6} = ip_0\bar{A}_0^3 - \sqrt{3}ip_0\bar{A}_0^8\\
&(D^{-1})_{8,8} = p^2\\
&(D^{-1})_{9,9} = p^2 + \frac{1}{4}(\bar{A}_0^3)^2 + \frac{1}{12}(\bar{A}_0^8)^2 + \frac{1}{12}(\bar{A}_0^{15})^2 + \frac{1}{2\sqrt{3}}\bar{A}_0^3\bar{A}_0^8 + \frac{1}{2\sqrt{3}}\bar{A}_0^3\bar{A}_0^{15} + \frac{1}{6}\bar{A}_0^8\bar{A}_0^{15}\\
&(D^{-1})_{9,10} = ip_0\bar{A}_0^3 + \frac{i}{\sqrt{3}}p_0 + \bar{A}_0^8 + \frac{i}{\sqrt{3}}p_0\bar{A}_0^{15}\\
&(D^{-1})_{10,10} = p^2 + \frac{1}{4}(\bar{A}_0^3)^2 + \frac{1}{12}(\bar{A}_0^8)^2 + \frac{1}{12}(\bar{A}_0^{15})^2 + \frac{1}{2\sqrt{3}}\bar{A}_0^3\bar{A}_0^8 + \frac{1}{2\sqrt{3}}\bar{A}_0^3\bar{A}_0^{15} + \frac{1}{6}\bar{A}_0^8\bar{A}_0^{15}\\
&(D^{-1})_{10,9} = -ip_0\bar{A}_0^3 - \frac{i}{\sqrt{3}}p_0 + \bar{A}_0^8 - \frac{i}{\sqrt{3}}p_0\bar{A}_0^{15}
\end{aligned}
\tag{B3}
$$

$$
\begin{aligned}
&(D^{-1})_{11,11} = p^2 + \frac{1}{4}(\bar{A}_0^3)^2 + \frac{1}{12}(\bar{A}_0^8)^2 + \frac{1}{12}(\bar{A}_0^{15})^2 - \frac{1}{2\sqrt{3}}\bar{A}_0^3\bar{A}_0^8 - \frac{1}{2\sqrt{3}}\bar{A}_0^3\bar{A}_0^{15} + \frac{1}{6}\bar{A}_0^8\bar{A}_0^{15}\\
&(D^{-1})_{11,12} = -ip_0\bar{A}_0^3 + \frac{i}{\sqrt{3}}p_0 + \bar{A}_0^8 + \frac{i}{\sqrt{3}}p_0\bar{A}_0^{15}\\
&(D^{-1})_{12,12} = p^2 + \frac{1}{4}(\bar{A}_0^3)^2 + \frac{1}{12}(\bar{A}_0^8)^2 + \frac{1}{12}(\bar{A}_0^{15})^2 - \frac{1}{2\sqrt{3}}\bar{A}_0^3\bar{A}_0^8 - \frac{1}{2\sqrt{3}}\bar{A}_0^3\bar{A}_0^{15} + \frac{1}{6}\bar{A}_0^8\bar{A}_0^{15}\\
&(D^{-1})_{12,11} = ip_0\bar{A}_0^3 - \frac{i}{\sqrt{3}}p_0 + \bar{A}_0^8 - \frac{i}{\sqrt{3}}p_0\bar{A}_0^{15}\\
&(D^{-1})_{13,13} = p^2 + \frac{1}{12}(\bar{A}_0^8)^2 + \frac{1}{12}(\bar{A}_0^{15})^2 - \frac{1}{6}\bar{A}_0^8\bar{A}_0^{15} (D^{-1})_{13,14} = -ip_0\bar{A}_0^8 + \frac{i}{\sqrt{3}}p_0\bar{A}_0^{15}\\
&(D^{-1})_{14,14} = p^2 + \frac{1}{12}(\bar{A}_0^8)^2 + \frac{1}{12}(\bar{A}_0^{15})^2 - \frac{1}{6}\bar{A}_0^8\bar{A}_0^{15} (D^{-1})_{14,13} = ip_0\bar{A}_0^8 - \frac{i}{\sqrt{3}}p_0\bar{A}_0^{15}\\
&(D^{-1})_{15,15} = p^2
\end{aligned}
\tag{B4}
$$

It is observed that the 15×15 propagator matrix in the color space $D^{-1}_{a,b}$ is a block diagonal matrix, consisting of three diagonal elements p^2 corresponding to the Cartan part and six 2×2 submatrices corresponding to the non-Cartan parts. Concretely, these six matrices are

$$
M_i = \begin{bmatrix} p_0^2 + \tilde{A}_i^2 - |\vec{p}|^2 & ip_0\tilde{A}_i \\ -ip_0\tilde{A}_i & p_0^2 + \tilde{A}_i^2 - |\vec{p}|^2 \end{bmatrix}, \tag{B5}
$$

where $\tilde{A}_i$ is a combination of A_0. From this expression we can see that the eigenvalues of M_i must be $(p_0 + A_i)^2 - |\vec{p}|^2$ and $(p_0 + A_i)^2 + |\vec{p}|^2$. After a unitary diagonalization we can get $\tilde{D}^{-1} \equiv U^\dagger D^{-1} U$ as

$$
\begin{aligned}
&(\tilde{D}^{-1})_{1,1} = (p_0 - \bar{A}_0^3)^2 - |\vec{p}|^2, \qquad (\tilde{D}^{-1})_{2,2} = (p_0 + \bar{A}_0^3)^2 - |\vec{p}|^2 \\
&(\tilde{D}^{-1})_{3,3} = (\tilde{D}^{-1})_{8,8} = (\tilde{D}^{-1})_{15,15} = p^2 \\
&(\tilde{D}^{-1})_{4,4} = \left[p_0 - \frac{1}{2}(\bar{A}_0^3 + \sqrt{3}\bar{A}_0^8)\right]^2 - |\vec{p}|^2, \qquad (\tilde{D}^{-1})_{5,5} = \left[p_0 + \frac{1}{2}(\bar{A}_0^3 + \sqrt{3}\bar{A}_0^8)\right]^2 - |\vec{p}|^2 \\
&(\tilde{D}^{-1})_{6,6} = \left[p_0 + \frac{1}{2}(\bar{A}_0^3 - \sqrt{3}\bar{A}_0^8)\right]^2 - |\vec{p}|^2, \qquad (\tilde{D}^{-1})_{7,7} = \left[p_0 - \frac{1}{2}(\bar{A}_0^3 - \sqrt{3}\bar{A}_0^8)\right]^2 - |\vec{p}|^2 \\
&(\tilde{D}^{-1})_{9,9} = \left[p_0 - \frac{1}{2}\left(\bar{A}_0^3 + \frac{1}{\sqrt{3}}\bar{A}_0^8 + \frac{1}{\sqrt{3}}\bar{A}_0^{15}\right)\right]^2 - |\vec{p}|^2 \\
&(\tilde{D}^{-1})_{10,10} = \left[p_0 + \frac{1}{2}\left(\bar{A}_0^3 + \frac{1}{\sqrt{3}}\bar{A}_0^8 + \frac{1}{\sqrt{3}}\bar{A}_0^{15}\right)\right]^2 - |\vec{p}|^2 \\
&(\tilde{D}^{-1})_{11,11} = \left[p_0 + \frac{1}{2}\left(\bar{A}_0^3 - \frac{1}{\sqrt{3}}\bar{A}_0^8 - \frac{1}{\sqrt{3}}\bar{A}_0^{15}\right)\right]^2 - |\vec{p}|^2 \\
&(\tilde{D}^{-1})_{12,12} = \left[p_0 - \frac{1}{2}\left(\bar{A}_0^3 - \frac{1}{\sqrt{3}}\bar{A}_0^8 - \frac{1}{\sqrt{3}}\bar{A}_0^{15}\right)\right]^2 - |\vec{p}|^2 \\
&(\tilde{D}^{-1})_{13,13} = \left(p_0 - \frac{1}{2}\frac{\bar{A}_0^8 - \bar{A}_0^{15}}{\sqrt{3}}\right)^2 - |\vec{p}|^2, \qquad (\tilde{D}^{-1})_{14,14} = \left(p_0 + \frac{1}{2}\frac{\bar{A}_0^8 - \bar{A}_0^{15}}{\sqrt{3}}\right)^2 - |\vec{p}|^2.
\end{aligned} \tag{B6}
$$

This leads to the quadratic Lagrangian written as

$$
\mathcal{L} = -\frac{1}{2}\tilde{A}_\mu^a(\tilde{D}^{-1})_a\tilde{A}^{\mu,a}, \tag{B7}
$$

with $\tilde{D}^{-1} = \mathrm{diag}((p_0 + A_1)^2 - |\vec{p}|^2, (p_0 + A_2)^2 - |\vec{p}|^2, \ldots, (p_0 + A_{15})^2 - |\vec{p}|^2) = \mathrm{diag}\{(p_0 + A_a)^2 - |\vec{p}|^2\}$ where A_a is zero or opposite numbers appearing in pairs. This structure is insured by the structural constant f_{abc}. One can check this structure for other $SU(N)$ theory. For example in $SU(3)$, the diagonal propagator is the same as the first eight propagators of $SU(4)$.

APPENDIX C: SUMMATION OVER THE THERMAL MODES

In this appendix we explicitly implement the summation over the thermal modes present in Eq. (3.11), rewritten as

$$
\log Z = 2V\mathrm{tr}_c \int \frac{d^3\vec{p}}{(2\pi)^2}\nu(E_g), \tag{C1}
$$

where we have introduced the function

$$
\nu(E_g) \equiv \sum_{n=-\infty}^{\infty} \log[\tilde{D}_{aa}^{-1}] = \sum_{n=-\infty}^{\infty} \log[(\omega_n - A_a)^2 + E_g^2], \tag{C2}
$$

with $E_g^2 = |\vec{p}|^2 + M_g^2$. To pull out the object to be summed from the logarithm, we differentiate $\nu(E_g)$ with respect to E_g,

$$
\begin{aligned}
\frac{\partial\nu(E_g)}{\partial E_g} &= \sum_{n=-\infty}^{\infty} \frac{2E_g}{(\omega_n - A_a)^2 + E_g^2} \\
&= \frac{1}{\pi T}\sum_{n=-\infty}^{\infty} \frac{E_g/2\pi T}{(n - A_a/2\pi T)^2 + (E_g/2\pi T)^2}.
\end{aligned} \tag{C3}
$$

Such a series can be summed explicitly, to get

$$
\begin{aligned}
\frac{\partial\nu(E_g)}{\partial E_g} &= \frac{1}{T}\frac{\sinh^2(E_g/2\pi T)}{\sin^2(A_a/2\pi T) + \sinh^2(E_g/2\pi T)} \\
&\quad \times \left(1 + \frac{e^{-E_g/T}}{1 - e^{-E_g/T}}\right).
\end{aligned} \tag{C4}
$$

Then, integrating both sides over E_g, we have

$$
\begin{aligned}
\nu(E_g) &= \frac{E_g}{T} + 2\log\left[\sqrt{\left(1 - e^{-i\frac{A_a}{T}}e^{\frac{-E_g}{T}}\right)\left(1 - e^{i\frac{A_a}{T}}e^{\frac{-E_g}{T}}\right)}\right] \\
&\quad + (E_g\,\text{independent terms}).
\end{aligned} \tag{C5}
$$

Using the identity $\log M = \log\det M$ and the fact that $\nu(E_g)$ is a diagonal matrix in the color space thus a simple trace operation, we obtain

$$
\begin{aligned}
\log Z &= 2V\int \frac{d^3\vec{p}}{(2\pi)^2} \\
&\quad \times 2\log\prod_a\left[\sqrt{\left(1 - e^{-i\frac{A_a}{T}}e^{\frac{-E_g}{T}}\right)\left(1 - e^{i\frac{A_a}{T}}e^{\frac{-E_g}{T}}\right)}\right],
\end{aligned} \tag{C6}
$$

where we have ignored the infinite vacuum energy and E_g independent terms. One should notice that each A_a is paired with another $A_b = -A_a$. Eventually, the generating function can be written as a more compacted form:

$$\log Z = 4V\mathrm{tr_c}\int \frac{d^3\vec{p}}{(2\pi)^2}\log\left(1-\hat{L}_A e^{-E_g/T}\right), \tag{C7}$$

with $\hat{L}_A = \mathrm{diag}(\exp(-iA_1/T), \exp(-iA_2/T), \ldots, \exp(-iA_{N^2-1}/T))$ where, again, $\pm A_a$ pairwise appear.

[1] Z. Kang, J. Zhu, and S. Matsuzaki, Dark confinement-deconfinement phase transition: A roadmap from Polyakov loop models to gravitational waves, J. High Energy Phys. 09 (2021) 060.

[2] J. Halverson, C. Long, A. Maiti, B. Nelson, and G. Salinas, Gravitational waves from dark Yang-Mills sectors, J. High Energy Phys. 05 (2021) 154.

[3] J. Kubo and M. Yamada, Scale and confinement phase transitions in scale invariant $SU(N)$ scalar gauge theory, J. High Energy Phys. 10 (2018) 003.

[4] W. C. Huang, M. Reichert, F. Sannino, and Z. W. Wang, Testing the dark $SU(N)$ Yang-Mills theory confined landscape: From the lattice to gravitational waves, Phys. Rev. D **104**, 035005 (2021).

[5] A. J. Helmboldt, J. Kubo, and S. van der Woude, Observational prospects for gravitational waves from hidden or dark chiral phase transitions, Phys. Rev. D **100**, 055025 (2019).

[6] C. Caprini, M. Hindmarsh, S. Huber, T. Konstandin, J. Kozaczuk, G. Nardini, J. M. No, A. Petiteau, P. Schwaller, G. Servant *et al.*, Science with the space-based interferometer eLISA. II: Gravitational waves from cosmological phase transitions, J. Cosmol. Astropart. Phys. 04 (2016) 001.

[7] H. An, S. L. Chen, R. N. Mohapatra, and Y. Zhang, Leptogenesis as a common origin for matter and dark matter, J. High Energy Phys. 03 (2010) 124.

[8] Z. Chacko, H. S. Goh, and R. Harnik, Natural Electroweak Breaking from a Mirror Symmetry, Phys. Rev. Lett. **96**, 231802 (2006).

[9] R. Blumenhagen, M. Cvetic, P. Langacker, and G. Shiu, Toward realistic intersecting D-Brane models, Annu. Rev. Nucl. Part. Sci. **55**, 71 (2005).

[10] Z. Kang, Slightly ultra-violet freeze-in a hidden gluonic sector, Phys. Lett. B **801**, 135149 (2020).

[11] P. Carenza, R. Pasechnik, G. Salinas, and Z. W. Wang, Glueball Dark Matter Revisited, Phys. Rev. Lett. **129**, 261302 (2022).

[12] F. Sannino, Polyakov loops versus hadronic states, Phys. Rev. D **66**, 034013 (2002).

[13] E. Morgante, N. Ramberg, and P. Schwaller, Gravitational waves from dark $SU(3)$ Yang-Mills theory, Phys. Rev. D **107**, 036010 (2023).

[14] S. He, L. Li, Z. Li, and S. J. Wang, Gravitational waves and primordial black hole productions from gluodynamics, arXiv:2210.14094.

[15] C. Ratti, M. A. Thaler, and W. Weise, Phase diagram and thermodynamics of the PNJL model, arXiv:nucl-th/0604025.

[16] R. D. Pisarski, Tests of the Polyakov loops model, Nucl. Phys. **A702**, 151 (2002).

[17] K. Fukushima and V. Skokov, Polyakov loop modeling for hot QCD, Prog. Part. Nucl. Phys. **96**, 154 (2017).

[18] S. Roessner, C. Ratti, and W. Weise, Polyakov loop, diquarks, and the two-flavor phase diagram, Phys. Rev. D **75**, 034007 (2007).

[19] K. Fukushima, Chiral effective model with the Polyakov loop, Phys. Lett. B **591**, 277 (2004).

[20] K. Fukushima, Phase diagrams in the three-flavor Nambu–Jona-Lasinio model with the Polyakov loop, Phys. Rev. D **77**, 114028 (2008); **78**, 039902(E) (2008).

[21] A. Mocsy, F. Sannino, and K. Tuominen, Confinement versus Chiral Symmetry, Phys. Rev. Lett. **92**, 182302 (2004).

[22] P. N. Meisinger, T. R. Miller, and M. C. Ogilvie, Phenomenological equations of state for the quark-gluon plasma, Phys. Rev. D **65**, 034009 (2002).

[23] P. N. Meisinger, M. C. Ogilvie, and T. R. Miller, Gluon quasiparticles and the Polyakov loop, Phys. Lett. B **585**, 149 (2004).

[24] A. Dumitru, Y. Guo, Y. Hidaka, C. P. K. Altes, and R. D. Pisarski, How wide is the transition to deconfinement?, Phys. Rev. D **83**, 034022 (2011).

[25] A. Dumitru, Y. Guo, Y. Hidaka, C. P. K. Altes, and R. D. Pisarski, Effective matrix model for deconfinement in pure gauge theories, Phys. Rev. D **86**, 105017 (2012).

[26] J. O. Andersen, E. Braaten, and M. Strickland, Hard-Thermal-Loop Resummation of the Free Energy of a Hot Gluon Plasma, Phys. Rev. Lett. **83**, 2139 (1999); Massive basketball diagram for a thermal scalar field theory, Phys. Rev. D **62**, 045004 (2000); J. O. Andersen, E. Braaten, E. Petitgirard, and M. Strickland, Hard-thermal-loop perturbation theory to two loops, Phys. Rev. D **66**, 085016 (2002).

[27] V. Goloviznin and H. Satz, The refractive properties of the gluon plasma in $SU(2)$ gauge theory, Z. Phys. C **57**, 671 (1993).

[28] A. Peshier, B. Kampfer, O. P. Pavlenko, and G. Soff, An effective model of the quark-gluon plasma with thermal parton masses, Phys. Lett. B **337**, 235 (1994).
[29] A. Peshier, B. Kampfer, O. P. Pavlenko, and G. Soff, Massive quasiparticle model of the $SU(3)$ gluon plasma, Phys. Rev. D **54**, 2399 (1996).
[30] M. I. Gorenstein and S. N. Yang, Gluon plasma with a medium-dependent dispersion relation, Phys. Rev. D **52**, 5206 (1995).
[31] C. Sasaki and K. Redlich, Effective gluon potential and hybrid approach to Yang-Mills thermodynamics, Phys. Rev. D **86**, 014007 (2012).
[32] M. Ruggieri, P. Alba, P. Castorina, S. Plumari, C. Ratti, and V. Greco, Polyakov loop and gluon quasiparticles in Yang-Mills thermodynamics, Phys. Rev. D **86**, 054007 (2012).
[33] C. A. Islam, M. G. Mustafa, R. Ray, and P. Singha, Consistent approach to study gluon quasiparticles, Phys. Rev. D **106**, 054002 (2022).
[34] G. Curci and R. Ferrari, On a class of Lagrangian models for massive and massless Yang-mills fields, Nuovo Cimento Soc. Ital. Fis. **32A**, 151 (1976).
[35] U. Reinosa, J. Serreau, M. Tissier, and N. Wschebor, Deconfinement transition in $SU(N)$ theories from perturbation theory, Phys. Lett. B **742**, 61 (2015).
[36] D. M. van Egmond, U. Reinosa, J. Serreau, and M. Tissier, A novel background field approach to the confinement-deconfinement transition, SciPost Phys. **12**, 087 (2022).
[37] U. Reinosa, J. Serreau, M. Tissier, and N. Wschebor, Deconfinement transition in $SU(2)$ Yang-Mills theory: A two-loop study, Phys. Rev. D **91**, 045035 (2015).
[38] U. Reinosa, J. Serreau, M. Tissier, and N. Wschebor, Two-loop study of the deconfinement transition in Yang-Mills theories: $SU(3)$ and beyond, Phys. Rev. D **93**, 105002 (2016).
[39] J. O. Andersen, M. Strickland, and N. Su, Gluon Thermodynamics at Intermediate Coupling, Phys. Rev. Lett. **104**, 122003 (2010).
[40] J. O. Andersen, L. E. Leganger, M. Strickland, and N. Su, NNLO hard-thermal-loop thermodynamics for QCD, Phys. Lett. B **696**, 468 (2011).
[41] R. A. Schneider and W. Weise, Quasiparticle description of lattice QCD thermodynamics, Phys. Rev. C **64**, 055201 (2001).
[42] P. Castorina, D. E. Miller, and H. Satz, Trace anomaly and quasi-particles in finite temperature $SU(N)$ gauge theory, Eur. Phys. J. C **71**, 1673 (2011).
[43] P. Castorina, V. Greco, D. Jaccarino, and D. Zappala, A reanalysis of finite temperature $SU(N)$ gauge theory, Eur. Phys. J. C **71**, 1826 (2011).
[44] N. Weiss, Effective potential for the order parameter of gauge theories at finite temperature, Phys. Rev. D **24**, 475 (1981).
[45] P. Alba, W. Alberico, M. Bluhm, V. Greco, C. Ratti, and M. Ruggieri, Polyakov loop and gluon quasiparticles: A self-consistent approach to Yang–Mills thermodynamics, Nucl. Phys. **A934**, 41 (2014).
[46] P. M. Lo, K. Redlich, and C. Sasaki, Fluctuations of the order parameter in an SU(Nc) effective model, Phys. Rev. D **103**, 074026 (2021).
[47] V. N. Gribov, Quantization of non-Abelian gauge theories, Nucl. Phys. **B139**, 1 (1978).
[48] J. Heffner, H. Reinhardt, and D. R. Campagnari, Deconfinement phase transition in the Hamiltonian approach to Yang-Mills theory in Coulomb gauge, Phys. Rev. D **85**, 125029 (2012).
[49] P. N. Meisinger and M. C. Ogilvie, Complete high temperature expansions for one-loop finite temperature effects, Phys. Rev. D **65**, 056013 (2002).
[50] U. Reinosa, *Perturbative Aspects of the Deconfinement Transition—Physics Beyond the Faddeev-Popov Model* (Springer, Cham, 2022), 10.1007/978-3-031-11375-8.
[51] Y. B. Ivanov, V. V. Skokov, and V. D. Toneev, Equation of state of deconfined matter within a dynamical quasiparticle description, Phys. Rev. D **71**, 014005 (2005).
[52] R. D. Pisarski, Effective theory of Wilson lines and deconfinement, Phys. Rev. D **74**, 121703 (2006).
[53] S. Datta and S. Gupta, Continuum thermodynamics of the SU(Nc) gluon plasma, Phys. Rev. D **82**, 114505 (2010).
[54] M. Raissi and P. Perdikaris, and G. E. Karniadakis, Physics-informed neural networks: A deep learning framework for solving forward and inverse problems involving nonlinear partial differential equations, J. Comput. Phys. **378**, 686 (2019).
[55] M. Abadi, P. Barham, J. Chen, Z. Chen, A. Davis, J. Dean *et al.*, TensorFlow: A system for large-scale machine learning, in *Proceedings of the 12th USENIX Conference on Operating Systems Design and Implementation, OSDI'16* (USENIX Association, USA, 2016), p. 265–283.
[56] J. Braun, H. Gies, and J. M. Pawlowski, Quark confinement from colour confinement, Phys. Lett. B **684**, 262 (2010).
[57] F. P. Li, H. L. Lü, L. G. Pang, and G. Y. Qin, Deep-learning quasi-particle masses from QCD equation of state, arXiv:2211.07994.